

Binuclear rhodium alkyl and acyl A-frame complexes: synthesis, structure and reactivity

Faisal Shafiq, Kurt W. Kramarz and Richard Eisenberg*

Department of Chemistry, University of Rochester, Rochester, NY 14627 (USA)

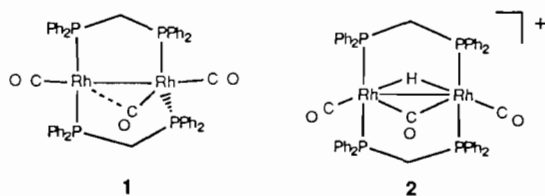
(Received March 19, 1993; revised June 18, 1993)

Abstract

The electrophilic alkylation of $\text{Rh}_2(\text{CO})_3(\text{dppm})_2$ (**2**) with $\text{CH}_3\text{SO}_3\text{CF}_3$ yields the μ -acyl A-frame complex $\text{Rh}_2(\mu\text{-CH}_3\text{CO})(\text{CO})_2(\text{dppm})_2^+$ (**3**). Complex **3** is unstable and at 70 °C forms the A-frame species $\text{Rh}_2(\text{CH}_3)(\mu\text{-CO})(\text{CO})(\text{dppm})_2^+$ (**4**) via CO loss. Between 40 and 70 °C, both complexes **3** and **4** are observed in solution. Complex **3** reacts with CO to yield the terminal acyl complex $\text{Rh}_2(\text{CH}_3\text{CO})(\text{CO})_3(\text{dppm})_2^+$ generated *in situ*. The characterization of complexes **3**, **4** and $\text{Rh}_2(\text{CH}_3\text{CO})(\text{CO})_3(\text{dppm})_2^+$ is based on NMR and IR spectroscopies, and single crystal X-ray diffraction methods for complexes **3** and **4**. The crystals of **3** are monoclinic (space group $P2_1/c$) having a unit cell of dimensions $a = 11.953(3)$, $b = 24.127(7)$, $c = 22.490(12)$ Å, $\beta = 103.00(3)^\circ$, $V = 6310.1$ Å³ and $Z = 4$, with one molecule per asymmetric unit along with acetone and diethyl ether as solvents of crystallization. Complex **3** possesses an A-frame structure in which the Rh centers are bridged by two dppm ligands, and an acyl group occupies the bridgehead position with the carbonyl carbon bonded to Rh1 and the oxygen bonded to Rh2. The Rh–Rh separation of 2.952(3) Å suggests a weak Rh–Rh interaction and the absence of a formal Rh–Rh single bond. The crystals of **4** are monoclinic (space group $P2_1/n$) having a unit cell of dimensions $a = 13.919(4)$, $b = 15.682(3)$, $c = 23.758(9)$ Å, $\beta = 96.76(3)^\circ$, $V = 5149.8$ Å³ and $Z = 4$, with one molecule per asymmetric unit. Complex **4** possesses an unsymmetrical A-frame structure with the two Rh centers bridged by two dppm ligands and CO located in the bridgehead position. The Rh–Rh bond distance is 2.811(2) Å. The reactivity of these complexes with H₂, phenyl acetylene and CO is also examined.

Introduction

The synthesis and reactivity of dppm (dppm = bis(diphenylphosphino)methane) bridged binuclear A-frame systems have been of long-standing interest in our laboratory and to others with regard to the reactivity of these systems with small molecules such as H₂ and CO [1–9]. Recently, we described the carbonylation of alkyl A-frame complexes $\text{Rh}_2(\mu\text{-CO})\text{R}_2(\text{dppm})_2$ (R = Me, Bz) leading to the formation of ketone and dione products by distinctly different and competitive pathways. Ketone products were generated by an intramolecular mechanism while dione products formed via a radical pathway. In each case, the sole metal containing product was $\text{Rh}_2(\text{CO})_3(\text{dppm})_2$ (**1**) [1, 20]



*Author to whom correspondence should be addressed.

The tricarbonyl complex **1** was originally synthesized in the BH_4^- reduction of $\text{Rh}_2\text{Cl}_2(\text{CO})_2(\text{dppm})_2$ under CO and was characterized as having a distinctly non-A-frame structure with a semi-bridging CO ligand and different coordination geometries at each of the Rh atoms [21]. Complex **1** reacts readily with H⁺ leading to the binuclear hydrido carbonyl complex $\text{Rh}_2(\mu\text{-H})(\mu\text{-CO})(\text{CO})_2(\text{dppm})_2^+$ (**2**), which has been characterized crystallographically [2]. In view of the reactivity of **1** with H⁺ and other electrophilic reagents and the carbonylation chemistry of $\text{Rh}_2(\mu\text{-CO})\text{R}_2(\text{dppm})_2$ (R = Me, Bz) leading to ketone and dione products, we undertook an investigation of the reaction chemistry of **1** with alkylating agents and subsequent carbonylation.

In the present paper we report the electrophilic alkylation of the tricarbonyl complex $\text{Rh}_2(\text{CO})_3(\text{dppm})_2$ (**1**) with methyl triflate, $\text{CH}_3\text{SO}_3\text{CF}_3$, to yield the new A-frame complex $\text{Rh}_2(\mu\text{-CH}_3\text{CO})(\text{CO})_2(\text{dppm})_2^+$ (**3**), which upon heating forms $\text{Rh}_2(\text{CH}_3)(\text{CO})_2(\text{dppm})_2^+$ (**4**) via carbonyl deinsertion and loss of CO. We also find that complex **3** reacts with excess CO to generate $\text{Rh}_2(\text{CH}_3\text{CO})(\text{CO})_3(\text{dppm})_2^+$ *in situ*.

Experimental

Materials, methods and preparations

Rhodium trichloride trihydrate (Johnson-Matthey) and the ligand dppm (bis(diphenylphosphino)methane) (Strem) were used as received without further purification. The starting complexes $\text{Rh}_2(\text{CO})_3(\text{dppm})_2$ and $\text{Rh}_2\text{Cl}_2(\text{CO})_2(\text{dppm})_2$ were prepared according to published procedures [21, 22]. All syntheses were performed under N_2 using standard Schlenk and inert atmosphere techniques. All solvents used were of reagent grade quality and were dried and degassed before use. THF- d_8 and C_6D_6 were dried with Na-benzophenone ketyl and vacuum distilled. CD_2Cl_2 was dried with CaH_2 prior to vacuum distillation. IR spectra were obtained on a Mattson 6020 Galaxy series FTIR spectrometer. ^1H and $^{31}\text{P}\{^1\text{H}\}$ NMR spectra were recorded on a Bruker AMX-400 spectrometer at field strengths of 400.13 and 161.92 MHz, respectively. Chemical shifts for ^1H NMR are reported in ppm downfield from tetramethylsilane, but were measured relative to residual ^1H resonances in the deuterated solvents (CH_2Cl_2 , δ 5.32 ppm; C_6D_6 , δ 7.15 ppm; THF- d_7 , δ 3.65 ppm). $^{31}\text{P}\{^1\text{H}\}$ chemical shifts are reported in ppm downfield from phosphoric acid, and were referenced to external 85% H_3PO_4 .

Preparation of compounds

$[\text{Rh}_2(\mu\text{-CH}_3\text{CO})(\text{CO})_2(\text{dppm})_2](\text{CF}_3\text{SO}_3)$ (3)

In a 50 ml round bottom flask, 0.130 g (119 μmol) of $\text{Rh}_2(\text{CO})_3(\text{dppm})_2$ (1) is dissolved in 10 ml of CH_2Cl_2 under an inert atmosphere. 75 μl (600 μmol) of neat $\text{CH}_3\text{SO}_3\text{CF}_3$ is injected into the solution and stirred at room temperature for 30 min. An immediate color change is observed as the dark red solution of $\text{Rh}_2(\text{CO})_3(\text{dppm})_2$ (1) reacts with methyl triflate to form a brilliant scarlet solution. The scarlet solution is cooled to -20°C and left for 0.5 h. Upon addition of excess cold Et_2O , complex 3 is precipitated and isolated as an air stable, deep purple solid. Yield 80%. Spectroscopic data: ^1H NMR (CD_2Cl_2 , ppm): δ 2.68 (broad; 2H; dppm $-\text{CH}_2-$), 3.62 (broad; 2H; dppm $-\text{CH}_2-$), 1.59 (s; 3H; μ -acyl), δ 7.15–7.80 (overlapping; 40H, dppm phenyls). $^{31}\text{P}\{^1\text{H}\}$ NMR: δ 20.41 and 23.6 ppm. IR (KBr, cm^{-1}): $\nu(\text{CO})=2006$ (terminal CO), 1989 (terminal CO), 1485 (μ -acyl); $\nu(^{13}\text{C})=1959$, 1943, 1429. $^{13}\text{C}\{^1\text{H}\}$ NMR (233 K, ppm): δ 322.0 (μ -acyl), δ 197.9 (terminal CO), 193.7 (terminal CO). *Anal.* Calc. for $\text{Rh}_2\text{P}_4\text{C}_{55}\text{H}_{47}\text{O}_6\text{SF}_3$: C, 54.03; H, 3.87. Found: C, 53.91; H, 3.93%.

$[\text{Rh}_2(\text{CH}_3)(\text{CO})_2(\text{dppm})_2](\text{CF}_3\text{SO}_3)$ (4)

In a 100 ml round bottom flask, 0.200 g of $\text{Rh}_2(\text{CO})_3(\text{dppm})_2$ (1) (183 μmol) is dissolved in 20 ml of C_6H_6 and placed under N_2 . 120 μl (960 μmol) of

neat $\text{CH}_3\text{SO}_3\text{CF}_3$ is then injected into the solution whereupon an immediate color change is observed as complex 3 is formed. This reaction mixture is then heated to 70°C under a N_2 purge to remove any liberated CO. After 2 h, the solvent is removed by evacuation. The orange solid which remains is recrystallized from $\text{CH}_2\text{Cl}_2/\text{Et}_2\text{O}$ and isolated as an orange air stable solid in 85% yield. Spectroscopic data: ^1H NMR (acetone- d_6 , ppm): δ 4.20 (mult; 2H; dppm $-\text{CH}_2-$), 4.43 (mult; 2H; dppm $-\text{CH}_2-$), 0.29 (quintet; $J=3.9$ Hz; 3H; CH_3), δ 7.34–7.62 (overlapping; 40H; dppm phenyl). $^{31}\text{P}\{^1\text{H}\}$ NMR: δ 28.00 ppm {AA'A''A'''XX' pattern; $J(^{103}\text{Rh}-^{31}\text{P})=123.7$ Hz}. IR (CH_2Cl_2 , cm^{-1}): $\nu(\text{CO})=2007$ (bridging), 1851 (terminal); $\nu(^{13}\text{C})=1961$, 1817. $^{13}\text{C}\{^1\text{H}\}$ NMR: δ 191.5 ppm ($J(^{103}\text{Rh}-^{31}\text{P})=64.59$ Hz). *Anal.* Calc. for $\text{Rh}_2\text{P}_4\text{C}_{54}\text{H}_{47}\text{O}_5\text{SF}_3 \cdot 1/2\text{CH}_2\text{Cl}_2$: C, 53.14; H, 3.89. Found: C, 53.51; H, 3.91%. The ^1H NMR spectrum of the elemental analysis sample was found to contain half an equivalent of CH_2Cl_2 .

In situ generation of

$[\text{Rh}_2(\text{CH}_3\text{CO})(\text{CO})_3(\text{dppm})_2](\text{CF}_3\text{SO}_3)$

In an NMR tube, 0.010 g (8 μmol) of complex 3 is dissolved in CD_2Cl_2 and placed under 1 atm. of CO. The solution turns from scarlet to red-orange immediately as $[\text{Rh}_2(\text{CH}_3\text{CO})(\text{CO})_3(\text{dppm})_2](\text{CF}_3\text{SO}_3)$ is formed. Spectroscopic data: ^1H NMR (CD_2Cl_2 , ppm): δ 3.83 (broad s; 4H; dppm $-\text{CH}_2-$), 0.75 (broad s; 3H; acyl). $^{31}\text{P}\{^1\text{H}\}$ NMR (233 K): δ 31.80, 15.82 ppm; $^{13}\text{C}\{^1\text{H}\}$ NMR (233 K, ppm): 189.2 (multiplet; terminal CO), 191.5 (broad; 2 terminal CO), 252.4 (acyl). IR (CH_2Cl_2 , cm^{-1}): $\nu(\text{CO})=2007$ (broad; terminal CO), 1641 (weak; acyl).

Reaction of 4 with H_2

0.010 g (9 μmol) of complex 4 is dissolved in CD_2Cl_2 and placed under 1 atm. of H_2 at room temperature. Immediate formation of the known complex $\text{Rh}_2(\mu\text{-H})(\text{CO})_2(\text{dppm})_2^+$ is observed based on comparison of NMR spectroscopic data with published results, along with the elimination of methane, appearing as a singlet at δ 0.21 ppm in the ^1H NMR spectrum [2].

Reaction of 4 with PhCCH

In an NMR tube 0.010 g (9 μmol) of complex 4 is dissolved in CD_2Cl_2 and then 20 μl of neat PhCCH is injected at room temperature. By ^1H NMR spectroscopy, the immediate formation of the known complex $\text{Rh}_2(\mu\text{-CCPh})(\text{CO})_2(\text{dppm})_2^+$ is observed along with the elimination of methane [23].

Reaction of $[\text{Rh}_2(\text{CH}_3\text{CO})(\text{CO})_3(\text{dppm})_2](\text{CF}_3\text{SO}_3)$ with H_2

In an NMR tube 0.010 g (7 μmol) of complex 3 is dissolved in CD_2Cl_2 and then placed under 1200 torr

of CO. The solution immediately turns orange as $[\text{Rh}_2(\text{CH}_3\text{CO})(\text{CO})_3(\text{dppm})_2](\text{CF}_3\text{SO}_3)$ is formed. This sample is then frozen and placed under 1 atm. of H_2 whereupon an immediate color change is observed as a dark red solution is formed. By ^1H NMR spectroscopy, a singlet at δ 9.74 ppm for acetaldehyde is observed along with the known complex $\text{Rh}_2(\mu\text{-CO})(\mu\text{-H})(\text{CO})_2(\text{dppm})_2^+$ [2]. When complex **3** is placed under 1200 torr of ^{13}CO , and then 1 atm. of H_2 , the acetaldehyde resonance at δ 9.74 in the ^1H NMR spectrum appears as a doublet with $J(^{13}\text{C}\text{-}^1\text{H})=172$ Hz.

Reaction of **3** with H_2

In an NMR tube, 0.010 g (7 μmol) of complex **3** is dissolved in CD_2Cl_2 and then placed under 1 atm. of H_2 at room temperature. By ^1H NMR spectroscopy, formation of methane as well as acetaldehyde is observed along with the formation of $\text{Rh}_2(\mu\text{-CO})(\mu\text{-H})(\text{CO})_2(\text{dppm})_2^+$ as evidenced by the appearance of singlets at δ 9.74 and 0.21 ppm for acetaldehyde and methane, respectively [2].

X-ray structure determinations of

$[\text{Rh}_2(\mu\text{-CH}_3\text{CO})(\text{CO})_2(\text{dppm})_2](\text{CH}_3\text{SO}_3)$ (**3**) and $[\text{Rh}_2(\mu\text{-CO})(\text{CO})(\text{CH}_3)(\text{dppm})_2](\text{CF}_3\text{SO}_3)$ (**4**)

Dark red crystals of complex **3** and orange–yellow crystals of complex **4** were grown from acetone/ Et_2O solution at -20 °C. Crystals of complex **3** with dimensions $0.6 \times 0.7 \times 0.5$ mm and complex **4** with dimensions $0.4 \times 0.5 \times 0.3$ mm were attached with epoxy to glass fibers on goniometer heads. Crystal data and data collection parameters for both structure determinations are summarized in Table 1. The initial cell determination for each crystal was carried out using 25 centered reflections from different parts of reciprocal space with θ between 5 and 13°. The cells were determined using the Enraf-Nonius CAD4-SDP peak search centering and indexing programs and were confirmed with the cell reduction program TRACER. The intensity data for both structure determinations showed no evidence of decay upon X-ray irradiation. Heavy atom methods were employed to locate the rhodium atoms in each determination and the DIRDIF program was used for structure expansion. Subsequent cycles of least-squares refinements and difference Fourier maps located the remaining non-hydrogen atoms. After isotropic refinement, an empirical absorption correction (DIFABS) was applied [24]. In the final refinements of complex **3**, all of the non-hydrogen atoms except C23, C29, C54, and those of the triflate anion and the solvents of crystallization were defined by anisotropic thermal parameters. For complex **4**, all non-hydrogen atoms except C52, C53 and O2 were assigned anisotropic thermal parameters, the atoms C52, C53 and O2 corresponded to the methyl and terminal CO ligands that

are disordered in the structure. The disorder in **4** was successfully treated by refining the occupancy factors of the disordered atoms while holding their isotropic thermal parameters fixed. For both structures, hydrogen atoms were placed in calculated positions around the phenyl rings and methyl groups. See also ‘Supplementary material’.

Results and discussion

Reaction of $\text{Rh}_2(\text{CO})_3(\text{dppm})_2$ (**1**) with methyl triflate

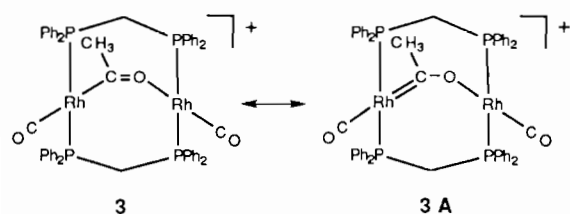
Reaction of the tricarbonyl complex $\text{Rh}_2(\text{CO})_3(\text{dppm})_2$ (**1**) with an excess of $\text{CH}_3\text{SO}_3\text{CF}_3$ in either CH_2Cl_2 , THF or acetone solution leads to an immediate color change and the generation of a new cationic species. Subsequent work up (*vide supra*) yields a purple, air stable product (80%, isolated yield) which is soluble in acetone, THF and CH_2Cl_2 and sparingly soluble in benzene. The ^1H NMR spectrum (CD_2Cl_2) of the purple solid exhibits characteristic resonances at δ 2.68 ppm and 3.62 ppm corresponding to inequivalent dppm $-\text{CH}_2-$ protons and a sharp resonance at δ 1.59 ppm assignable to the protons of a methyl group. When the sample is cooled to 273 K, the broad resonances of the dppm methylene protons resolve to multiplets. The methyl singlet at δ 1.59 ppm appears as a doublet with $J(^{13}\text{C}\text{-}^1\text{H})=4.1$ Hz in the ^{13}CO labeled analog of the complex and is therefore assigned as belonging to an acetyl group. The $^{13}\text{P}\{^1\text{H}\}$ NMR spectrum exhibits two sets of broad resonances at δ 20.41 and 23.60 ppm which upon cooling to 273 K also resolve into second order patterns. By IR spectroscopy, three bands are observed at 2006 (terminal CO), 1989 (terminal CO) and 1485 cm^{-1} . The IR stretch at 1485 cm^{-1} is too low for a terminal acetyl group and, based on experiments using ^{13}CO -labeled complex and ^{13}C NMR spectroscopy, is assigned as a bridging acetyl group. Specifically, when $1\text{-}^{13}\text{CO}$ is used in the reaction with methyl triflate, a resonance at δ 322.0 ppm is observed by ^{13}C NMR spectroscopy. This resonance is further downfield than conventional acyl carbonyl resonances which usually occur in the 230–260 ppm region of the spectrum and suggests that the acetyl carbon has carbene-like character. The terminal carbonyl resonances appear at δ 197.9 and 193.7 ppm, indicative of carbonyl ligand inequivalence.

Based on the spectroscopic data outlined above, we propose that the purple solid has the unsymmetrical A-frame structure shown as **3** in which the acetyl ligand forms a μ_2, η^2 -bridge with the acetyl carbon atom bonded to one rhodium center and the acetyl oxygen bonded to the other. This mode of coordination imparts carbene character to the acyl carbon via resonance structure

TABLE 1. Summary of crystallographic data for complexes **3** and **4**

	3	4
Empirical formula	C ₅₅ F ₃ H ₄₇ O ₆ P ₄ Rh ₂ S · C ₂ H ₆ O · C ₄ H ₁₀ O	C ₅₄ F ₃ H ₄₇ O ₅ P ₄ Rh ₂ S
Crystal system	monoclinic	monoclinic
Space group	<i>P2₁/c</i> (No. 14)	<i>P2₁/n</i> (No. 14)
<i>Z</i>	4	4
<i>a</i> (Å)	11.935(3)	13.919(4)
<i>b</i> (Å)	24.127(7)	15.682(3)
<i>c</i> (Å)	22.490(12)	23.757(9)
β (°)	103.00(3)	96.76(3)
<i>V</i> , Å ³	6310.14	5149.85
<i>D</i> _{calc} (g/cm ³)	1.4059	1.5369
<i>T</i> (°C)	−20.0	−20.0
Diffractometer	Enraf-Nonius CAD4	Enraf-Nonius CAD4
λ (Mo K α) (graphite monochromated radiation)	0.71069	0.71069
Scan type	2 θ / ω	2 θ / ω
Scan rate (°/min)	2–16.5	1–16.5
Total background time	scan time/2	scan time/2
Take-off angle (°)	2.6	2.6
Scan range (°)	0.7 + 0.35 tan θ	0.7 + 0.35 tan θ
2 θ Range (°)	4 < 2 θ < 40	4 < 2 θ < 40
Data collected	+ <i>h</i> , ± <i>k</i> , ± <i>l</i>	+ <i>h</i> , ± <i>k</i> , ± <i>l</i>
No. data collected	6456	5301
No. unique data > 3 σ	3145	2644
No. parameters varied	612	619
Absorption coefficient (cm ^{−1})	7.030	8.477
Systematic absences	<i>h</i> 0 <i>l</i> , <i>l</i> odd 0 <i>k</i> 0, <i>k</i> odd	<i>h</i> 0 <i>l</i> , <i>h</i> + <i>l</i> odd 0 <i>k</i> 0, <i>k</i> odd
Range transmission factors	0.712–1.194	0.916–1.058
Equivalent data	0 <i>kl</i> , 0 <i>k</i> \bar{l}	0 <i>kl</i> , 0 <i>k</i> \bar{l}
Agreement of equiv. data (<i>F</i> ₀)	0.014	0.061
<i>R</i> ₁	0.072	0.038
<i>R</i> ₂	0.079	0.038
Goodness of fit	2.40	1.22
Largest peak in final <i>E</i> map	1.29	0.397

3A. Confirmation of the structural assignment for **3** was obtained from a crystal structure determination.



Solid-state structure of

$[Rh_2(\mu\text{-CH}_3\text{CO})(CO)_2(dppm)_2](CF_3SO_3)$ (**3**)

The X-ray diffraction study showed complex **3** to possess the molecular structure given in Fig. 1. A summary of data collection parameters, crystallographic data and refinement information is given in Table 1. The complex crystallizes in the monoclinic space group *P2₁/c* with one independent binuclear complex per unit cell. The crystal structure is composed of discrete, well separated cations **3**, triflate anions, and acetone and ether solvents of crystallization. Selected intramolecular

distances and angles are tabulated in Tables 2 and 3. The molecular structure corresponds to an unsymmetrical A-frame arrangement with two approximately square planar rhodium centers bridged by two dppm ligands and an η^2 -acetyl group. A terminal carbonyl completes the coordination geometry for each rhodium center. The Rh1–Rh2 separation of 2.952(3) Å indicates the absence of a formal single bond between the Rh centers based on comparison with known systems containing Rh–Rh bonds [7, 16, 21, 25–29]. Each rhodium atom has two *trans* P donors (P1–Rh1–P4 = 165.9(2)° and P2–Rh2–P3 = 175.7(2)°). The bridging acetyl carbon atom C53 is approximately *trans* to the terminal CO ligand on Rh1 (C53–Rh1–C51 = 163.8(9)°), as is the acetyl oxygen O₃ on Rh2 (O3–Rh2–C52 = 171.5(8)°). The acetyl group lies on an approximate mirror plane which bisects the A-frame structure. The Rh2–O3 bond distance of 2.18 Å is slightly longer than that observed for Rh₂(μ -O)(dppm)₂ where the Rh–O distances were found to be 2.066(4) and 2.037(4) Å [30].

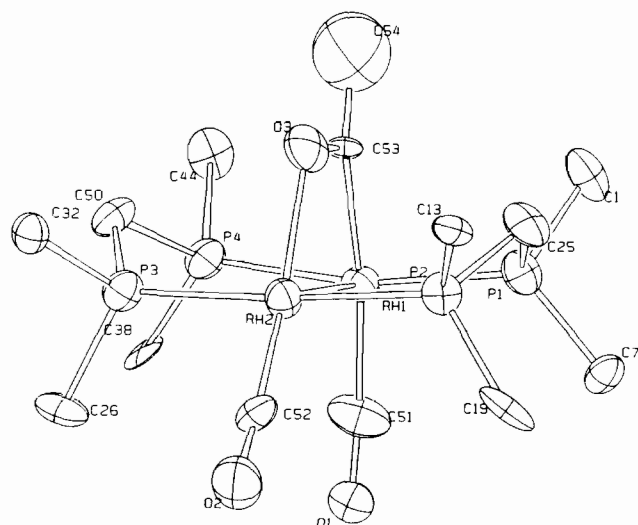


Fig. 1. A perspective view of $[\text{Rh}_2(\mu\text{-OCCH}_3)(\text{CO})_2(\text{dppm})_2]^+$ (**3**) showing the acyl group occupying the bridgehead position of the A-frame structure. Only the *ipso* carbons of the dppm phenyl rings are shown. The counterion CF_3SO_3^- and the remaining phenyl carbons have been omitted for clarity. Thermal ellipsoids are set at 35% probability.

TABLE 2. Intramolecular bond distances (Å) for $[\text{Rh}_2(\mu\text{-COCH}_3)(\text{CO})_2(\text{dppm})_2](\text{CF}_3\text{SO}_3)$ (**3**)

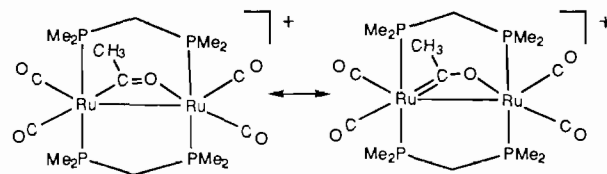
Rh1–Rh2	2.952(3)	P2–C19	1.82(2)
Rh1–P1	2.309(5)	P2–C25	1.86(2)
Rh1–P4	2.311(5)	P3–C26	1.86(2)
Rh1–C51	1.82(2)	P3–C32	1.82(2)
Rh1–C53	2.05(2)	P3–C50	1.80(2)
Rh2–P2	2.315(5)	P4–C38	1.81(2)
Rh2–P3	2.321(5)	P4–C44	1.84(2)
Rh2–O3	2.19(1)	P4–C50	1.91(2)
Rh2–C52	1.80(2)	O1–C51	1.17(2)
P1–C1	1.84(2)	O2–C52	1.16(2)
P1–C7	1.79(2)	O3–C53	1.28(2)
P1–C25	1.88(2)	C53–C54	1.39(3)
P2–C13	1.77(2)		

The most intriguing feature of **3** is the bonding in the bridging acyl group. Based on ^{13}C NMR spectroscopy discussed above that clearly shows a chemical shift consistent with carbene-like character, the oxy-carbene resonance structure **3A** was proposed. The C53–O3 bond distance of 1.28(2) Å and Rh1–C53 bond distance of 2.05(2) Å are consistent with that oxy-carbene description [31, 32]. A similar observation of carbenoid character in a bridging acyl ligand has been made by Johnson and Gladfelter in a related methylation reaction. Specifically, the reaction of the dmpm bridged binuclear complex $\text{Ru}_2(\text{CO})_5(\text{dmpm})_2$, where dmpm = bis(dimethylphosphino)methane, with methyl triflate leads to the acetyl bridged complex $\text{Ru}_2(\mu_2, \eta^2\text{-OCCH}_3)(\text{CO})_5(\text{dmpm})_2^+$, shown as **I**, as the major

TABLE 3. Intramolecular bond angles (°) for $[\text{Rh}_2(\mu\text{-COCH}_3)(\text{CO})_2(\text{dppm})_2](\text{CF}_3\text{SO}_3)$ (**3**)

Rh2–Rh1–P1	93.6(2)	C1–P1–C7	103(1)
Rh2–Rh1–P4	93.4(2)	C1–P1–C25	101(1)
Rh2–Rh1–C51	95.4(7)	C7–P1–C25	107.5(8)
Rh2–Rh1–C53	68.4(5)	Rh2–P2–C13	113.6(7)
P1–Rh1–P4	165.9(2)	Rh2–P2–C19	118.9(6)
P1–Rh1–C51	97.2(7)	Rh2–P2–C25	112.2(5)
P1–Rh1–C53	85.1(5)	C13–P2–C19	104.4(9)
P4–Rh1–C51	94.3(6)	C13–P2–C25	102.9(9)
P4–Rh1–C53	86.1(5)	C19–P2–C25	103(1)
C51–Rh1–C53	163.8(9)	Rh2–P3–C26	117.2(6)
Rh1–Rh2–P2	89.8(2)	Rh2–P3–C32	115.2(6)
Rh1–Rh2–P3	89.2(2)	Rh2–P3–C50	112.9(6)
Rh1–Rh2–O3	64.9(4)	C26–P3–C32	103(1)
Rh1–Rh2–C52	123.6(7)	C26–P3–C50	104.7(9)
P2–Rh2–P3	175.7(2)	C32–P3–C50	101.8(9)
P2–Rh2–O3	87.7(3)	Rh1–P4–C38	121.3(6)
P2–Rh2–C52	92.9(6)	Rh1–P4–C44	109.6(7)
P3–Rh2–O3	88.1(3)	Rh1–P4–C50	110.7(6)
P3–Rh2–C52	91.1(6)	C38–P4–C44	103.0(9)
O3–Rh2–C52	171.5(8)	C38–P4–C50	107.0(9)
Rh1–P1–C1	111.1(6)	C44–P4–C50	104(1)
Rh1–P1–C7	122.0(7)	P1–C25–P2	112(1)
Rh1–P1–C25	109.7(6)	P3–C50–P4	111.5(9)
Rh2–O3–C53	112(1)		
Rh1–C51–O1	172(2)		
Rh2–C52–O2	173(2)		
Rh1–C53–O3	115(1)		
Rh1–C53–C54	134(2)		
O3–C53–C54	110(2)		

product [**33**]. The acyl carbon in **I** exhibits a resonance at δ 293.8 ppm and was assigned carbenoid character.



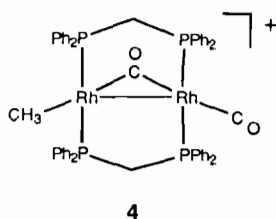
I

Reaction of $\text{Rh}_2(\text{CO})_3(\text{dppm})_2$ with methyl triflate at 70 °C

Reaction of the tricarbonyl complex $\text{Rh}_2(\text{CO})_3(\text{dppm})_2$ (**1**) with an excess of $\text{CH}_3\text{SO}_3\text{CF}_3$ in C_6H_6 initially forms a scarlet solution of complex **3**. However, upon heating at 70–80 °C under a N_2 purge, the solution turns bright orange after 2 h and an orange solid remains after C_6H_6 is removed under vacuum. The orange solid can be filtered in air and isolated in 85% yield. The new cationic species is soluble in acetone, THF and CH_2Cl_2 , and insoluble in Et_2O , hexanes and C_6H_6 . The ^1H NMR spectrum (acetone- d_6) exhibits resonances at δ 4.20 and 4.43 ppm arising from two sets of inequivalent dppm $-\text{CH}_2-$ protons and a quintet at δ 0.29 ppm corresponding to a methyl group. The splitting of the quintet at δ 0.29 ppm is due to coupling

of the methyl protons with four equivalent phosphorus nuclei; upon ^{31}P decoupling, only a sharp singlet is observed. The methyl resonance shows no additional coupling when ^{13}CO -labeled complex is prepared, indicating that the methyl group is not part of an acetyl ligand and is instead coordinated directly to the metal center.

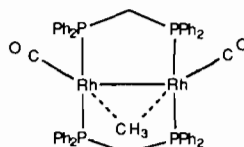
The $^{31}\text{P}\{^1\text{H}\}$ NMR spectrum of the orange solid exhibits a single symmetric second order pattern at δ 28.00 ppm (AA'A''A'''XX' pattern; $J(^{103}\text{Rh}-^{31}\text{P})=123.7$ Hz), while the spectrum obtained using ^{13}CO -labeled complex shows an additional splitting of the two most intense lines of the second order pattern. However, the ^{13}C NMR spectrum exhibits only a single terminal CO resonance at δ 191.5 ppm ($J(^{103}\text{Rh}-^{31}\text{P})=64.59$ Hz). By IR spectroscopy (CH_2Cl_2), two CO stretches are observed at 2007 and 1851 cm^{-1} which, upon ^{13}CO substitution, shift to 1961 and 1817 cm^{-1} . The spectroscopic observations described above can be rationalized by the existence of a fluxional binuclear complex in which terminal and bridging carbonyls are readily interconverted and the methyl ligand is rapidly exchanged between the two rhodium centers, yielding equivalent coupling of the methyl protons to the four ^{31}P nuclei of the dppm ligands. The static structure we propose for this complex which is consistent with the IR spectroscopic results and is confirmed by an X-ray structure determination, is a CO-bridged A-frame arrangement having one terminal carbonyl and one methyl ligand, **4**.



4

Attempts to probe the fluxional process in **4** that equilibrates the two carbonyl ligands and allows methyl migration between the two Rh centers were mostly unsuccessful. At 183 K, the $^{31}\text{P}\{^1\text{H}\}$ NMR spectrum coalesces to a broad and featureless resonance, consistent with carbonyl equilibration and methyl migration between metal centers. In the ^1H NMR spectrum at 183 K, the dppm $-\text{CH}_2-$ protons appear as a broad singlet instead of the two well resolved multiplets observed at room temperature. The latter observation is at first glance contradictory in that the methylene protons in the room temperature fast exchange limit show inequivalence while appearing to coalesce at low temperature. The result is rationalized by a simple difference in chemical shift temperature dependence of the two methylene resonances such that $\Delta\delta$ diminishes as temperature decreases. The inequivalence of the

dppm methylene protons at room temperature eliminates certain rearrangement mechanisms but is consistent with a simple methyl migration via structure **II**. Methyl migration between metal centers has only been observed for a few complexes and shown in some to proceed via C-H activated intermediate. Reported cases include $(\text{Cp})_2(\text{CH}_3)\text{TaPt}(\text{PMe}_3)_2(\mu\text{-CH}_2)$ [34], $\text{HOs}_3(\text{CO})_{10}(\text{CH}_3)$ [35], $\text{Ir}_2\text{H}(\text{CO})_3(\mu\text{-CH}_2)(\text{dppm})_2^+$ [36], $(\text{Cp}_2\text{CH}_2)\text{Co}_2(\text{CO})_2(\text{CH}_3)_2$ [37] and $[\text{Cp}^*\text{Rh}(\text{CO})(\text{CH}_3)]_2$ [38]. Recently Antwi-Nsiah and Cowie have reported that the related dppm bridged binuclear Rh-Ir and Ir-Ir systems undergo facile methyl migrations via an observed C-H activated intermediate which is only observed in the Ir-Ir analog [36]. However, in 1989 Kubiak and co-workers reported the synthesis and crystal structure of $\text{Ir}(\text{CO})_4(\text{dmpp})_2(\mu\text{-CH}_3)^+$ in which the methyl group symmetrically bridges the two metal centers [39]. We do not observe any intermediates with our Rh-Rh system.



II

Solid-state structure of $[\text{Rh}_2(\text{CH}_3)(\text{CO})_2(\text{dppm})_2](\text{CF}_3\text{SO}_3)$ (**4**)

A single crystal X-ray diffraction study established the A-frame geometry of complex **4** as shown in the perspective drawing of Fig. 2. The crystal structure consists of well separated binuclear complex cations and triflate anions. Selected intramolecular distances and angles are presented in Tables 4 and 5. The molecular structure of **4** is that of an A-frame with two dppm ligands and a single CO bridging the two Rh atoms. The phosphine donors at each Rh are mutually *trans* ($\text{P1-Rh1-P4}=172.1(1)^\circ$ and $\text{P2-Rh2-P3}=173.2(1)^\circ$). The Rh-Rh separation of 2.811(2) Å is consistent with an Rh-Rh single bond and compares well with Rh-Rh single bond distances in $\text{Rh}_2(\mu\text{-SiPhH})\text{H}_2(\text{CO})_2(\text{dppm})_2$ (2.813(1) Å), $\text{Rh}_2(\mu\text{-CO})\text{Br}_2(\text{dppm})_2$ (2.7566(8) Å), $\text{Rh}_2(\mu\text{-CF}_3\text{C}_2\text{CF}_3)\text{Cl}_2(\text{dppm})_2$ (2.7447(9) Å) and $\text{Rh}_2(\mu\text{-CO})(\text{CO})_2(\mu\text{-Cl})(\text{dppm})_2^+$ (2.7838(8) Å) [16, 19, 25, 29]. The bridging carbonyl is unsymmetrically positioned relative to the two Rh centers with an Rh1-C54 distance of 2.11(1) Å and an Rh2-C54 distance of 1.98(1) Å. The difference in these two values may be attributable to the nature of the other ligand besides bridging dppm attached to the Rh atoms, being terminal CO in the former case and methyl in the latter. However, in the

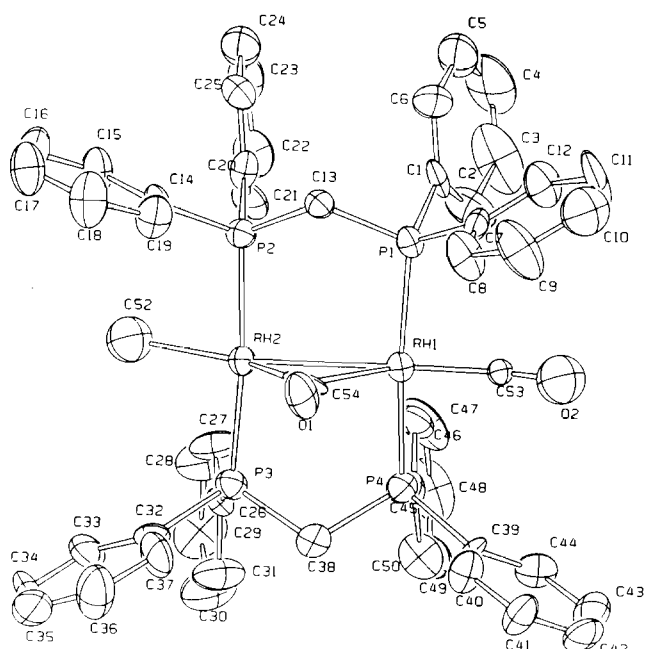


Fig. 2. A perspective view of $[\text{Rh}_2(\text{CH}_3)(\mu\text{-CO})(\text{CO})(\text{dppm})_2]^+$ (**4**) showing the CO group occupying the bridgehead position of the A-frame structure. The counterion CF_3SO_3^- has been omitted for clarity. Thermal ellipsoids are set at 50% probability.

TABLE 4. Intramolecular bond distances (Å) for $[\text{Rh}_2\text{CH}_3(\mu\text{-CO})(\text{CO})(\text{dppm})_2](\text{CF}_3\text{SO}_3)$ (**4**)

Rh1–Rh2	2.811(2)	P2–C13	1.82(1)
Rh1–P1	2.309(4)	P2–C14	1.83(1)
Rh1–P4	2.317(4)	P2–C20	1.83(1)
Rh1–C53	1.78(2)	P3–C26	1.81(1)
Rh1–C54	2.11(1)	P3–C32	1.83(1)
Rh2–P2	2.320(4)	P3–C38	1.84(1)
Rh2–P3	2.316(4)	P4–C38	1.84(1)
Rh2–C52	2.21(4)	P4–C39	1.83(1)
Rh2–C54	1.98(1)	P4–C45	1.83(1)
P1–C1	1.83(1)	O1–C54	1.13(1)
P1–C7	1.80(1)	O2–C53	1.13(2)
P1–C13	1.84(1)		

crystal the terminal carbonyl and methyl ligands exhibit disorder. Refinement of a model in which the occupancies of terminal CO and methyl positions were varied subject to the constraints that the total methyl and terminal CO populations are unity and that for each Rh center the terminal CO and methyl populations must sum to one yielding occupancy factors of 60 and 40%. This result means that Rh2 has a methyl group with a 60% occupancy factor and a terminal CO ligand with 40% occupancy while Rh1 has the same ligands with occupancy factors reversed. The rather similar occupancy factors (60:40) renders an explanation of the slight asymmetry of the bridging carbonyl based on 'trans' ligand suspect. (Because of the metal–metal bond, the bridging CO is not strictly *trans* to the terminal

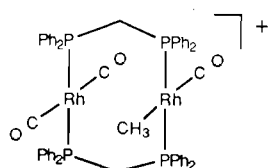
TABLE 5. Intramolecular bond angles (°) for $[\text{Rh}_2\text{CH}_3(\mu\text{-CO})(\text{CO})(\text{dppm})_2](\text{CF}_3\text{SO}_3)$ (**4**)

Rh2–Rh1–P1	93.28(9)	C1–P1–C7	104.3(6)
Rh2–Rh1–P4	90.9(1)	C1–P1–C13	105.1(6)
Rh2–Rh1–C53	175.6(7)	C7–P1–C13	104.7(5)
Rh2–Rh1–C54	44.8(4)	Rh2–P2–C13	113.0(4)
P1–Rh1–P4	172.1(1)	Rh2–P2–C14	114.0(4)
P1–Rh1–C53	88.1(6)	Rh2–P2–C20	116.1(5)
P1–Rh1–C54	91.8(3)	C13–P2–C14	103.5(5)
P4–Rh1–C53	87.3(6)	C13–P2–C20	104.7(5)
P4–Rh1–C54	95.9(3)	C14–P2–C20	104.2(6)
C53–Rh1–C54	139.4(7)	Rh2–P3–C26	116.8(4)
Rh1–Rh2–P2	91.7(1)	Rh2–P3–C32	115.0(4)
Rh1–Rh2–P3	93.91(9)	Rh2–P3–C38	112.6(4)
Rh1–Rh2–C52	160.5(8)	C26–P3–C32	103.4(6)
Rh1–Rh2–C54	48.6(4)	C26–P3–C38	104.7(5)
P2–Rh2–P3	173.2(1)	C32–P3–C38	103.0(5)
P2–Rh2–C52	84.7(8)	Rh1–P4–C38	113.4(4)
P2–Rh2–C54	92.1(3)	Rh1–P4–C39	115.1(4)
P3–Rh2–C52	88.7(8)	Rh1–P4–C45	110.7(4)
P3–Rh2–C54	94.5(3)	C38–P4–C39	101.9(5)
C52–Rh2–C54	150.5(9)	C38–P4–C45	106.5(5)
Rh1–P1–C1	115.6(5)	C39–P4–C45	108.5(6)
Rh1–P1–C7	113.6(4)	P1–C13–P2	111.0(5)
Rh1–P1–C13	112.5(4)	P3–C38–P4	109.8(5)
Rh1–C53–O2	164(2)		
Rh1–C54–Rh2	86.6(5)		
Rh1–C54–O1	131(1)		
Rh2–C54–O1	142(1)		

CO or methyl ligand with C54–Rh1–C53 of 139.4(7) and C54–Rh2–C52 of 150.5(9)°, respectively). We therefore have no explanation for the asymmetry of the bridging carbonyl in **4**, although in a statistical sense it appears to be real.

Reactions of **3**

From the results presented above, it is evident that **3** is formed initially in the reaction of **1** with methyl triflate and that upon heating at 70 °C loses CO and generates **4**. The formation of **3** probably proceeds via initial methylation at one of the Rh centers of **1**, generating an unobserved tricarbonyl methyl species $\text{Rh}_2\text{Me}(\text{CO})_3(\text{dppm})_2^+$ shown as **III** which undergoes carbonyl insertion to give **3** or loses CO to form **4**. This species is undoubtedly on the pathway for converting **3** to **4**, and the predominance of **3** when the methylation of **1** is carried out under CO underscores the facility of CO insertion relative to CO loss in this reaction system. If the conversion of **3** to **4** is carried in a closed system, i.e. if a solution of **3** is heated at 70 °C in a closed system, then conversion to **4** is reversible with **3** reforming upon cooling of the sample. The interconversion of **3** and **4** may proceed alternatively via initial CO dissociation and a carbonyl acetyl intermediate, but this seems less likely.



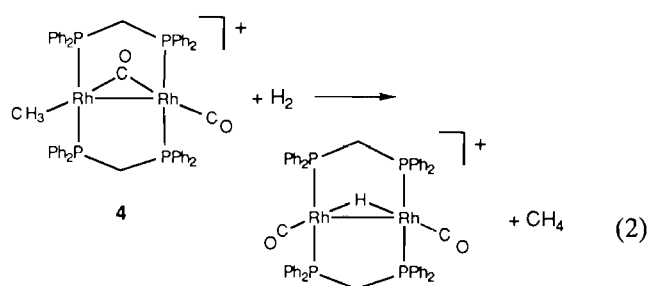
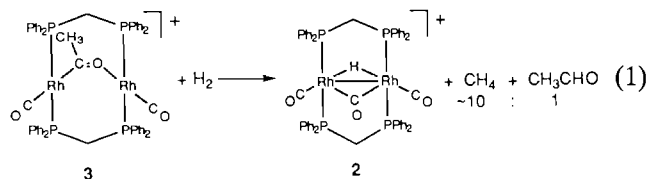
III

Complex **3** is also observed to react further with CO. When a CD_2Cl_2 solution of **3** is placed under 1 atm. of CO a new complex is formed. The room temperature ^1H NMR spectrum exhibits a set of broad resonances at δ 3.83 (broad s; 4H) and 0.75 (broad s; 3H) ppm while the aryl region is broad and featureless. By $^{31}\text{P}\{^1\text{H}\}$ NMR spectroscopy, two sets of broad resonances at δ 31.80 and 15.82 ppm are observed indicating inequivalent phosphorus nuclei. Upon cooling to 233 K, the ^1H NMR resonances for the dppm methylene and acyl groups sharpen but remain unstructured, while the aryl resonances appear as overlapping multiplets. The $^{31}\text{P}\{^1\text{H}\}$ resonances now appear as two highly structured second order patterns. The $^{13}\text{C}\{^1\text{H}\}$ NMR spectrum at 233 K exhibits three broad resonances at δ 252.4, 191.5 and 189.2 ppm, which integrate roughly as 1:2:1. The resonance at δ 252 ppm is typical of an acetyl carbon while the higher field resonances are in the terminal carbonyl region. The IR spectrum exhibits two stretches at 2007 and 1641 cm^{-1} . Upon ^{13}CO substitution, a band at 1943 cm^{-1} is observed, while the expected lower energy band is obscured by stretches due to other ligands. Based on these spectroscopic features, we formulate this new orange complex as $[\text{Rh}_2(\text{CH}_3\text{CO})(\text{CO})_3(\text{dppm})_2]^+$. The isolation of this species in pure form as its triflate salt has proven extremely difficult since it readily loses CO in the absence of an excess CO atmosphere and at temperatures above -78°C .

Reactions with H_2

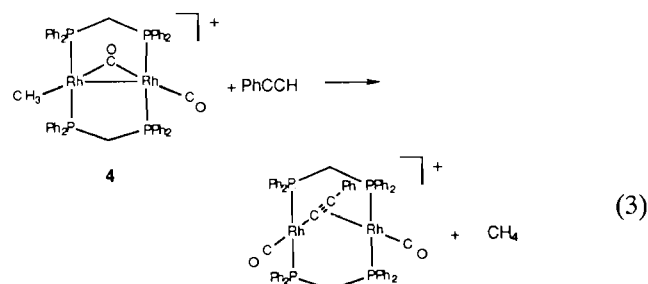
Complexes **3** and **4** are both found to react with H_2 . For complex **3**, the reaction under 1 atm. of H_2 in CD_2Cl_2 leads to the formation of methane and acetaldehyde in a 10:1 ratio as determined by ^1H NMR spectroscopy, while for complex **4**, only methane is observed as the organic product. In the former case shown as eqn. (1), the only observed metal containing product is the bridging hydride, bridging carbonyl, complex $\text{Rh}_2(\mu\text{-H})(\mu\text{-CO})(\text{CO})_2(\text{dppm})_2^+$ (**2**) [2] whereas for the latter, the metal containing product is the known bridging hydride complex $\text{Rh}_2(\mu\text{-H})(\text{CO})_2(\text{dppm})_2^+$ shown in eqn. (2). When the reaction with H_2 is conducted with the carbonylated complex $[\text{Rh}_2(\text{CH}_3\text{CO})(\text{CO})_3(\text{dppm})_2]^+$ generated *in situ* from **3** and 1 atm. of CO, only acetaldehyde and complex

2 are seen to form. The acetaldehyde product is identified by the characteristic aldehyde resonance at δ 9.74 ppm which changes to a doublet ($J(^{13}\text{C}\text{-}^1\text{H}) = 172$ Hz) when ^{13}CO -labeled complex is used. It is evident that the formation of methane and acetaldehyde arises via C-H reductive elimination from an alkyl or acyl hydride species. The fact that methane is the principal product when the reaction is run with the acetyl complex **3** underscores the facility of carbonyl deinsertion/insertion in its reaction chemistry.



Reaction of **4** with PhCCH

When an excess of phenylacetylene is added to an acetone- d_6 solution of complex **4**, an immediate color change from orange to red is observed. By ^1H and ^{31}P NMR spectroscopies, methane is found to be generated, and formation of the known phenylacetylide-bridged A-frame species $\text{Rh}_2(\sigma, \mu\text{-C}_2\text{Ph})(\text{CO})_2(\text{dppm})_2^+$ is seen to occur (eqn. (3)). Identification of the acetylide bridged complex was established by comparison of NMR data with that of an authentic sample originally reported by Deranlyagala and Grundy [23].



Conclusions

Electrophilic alkylation of the tricarbonyl complex $\text{Rh}_2(\text{CO})_3(\text{dppm})_2$ (**1**) with methyl triflate yields the new A-frame complex $\text{Rh}_2(\mu\text{-CH}_3\text{CO})(\text{CO})_2(\text{dppm})_2^+$ (**3**) via methylation at the metal center followed by

insertion of CO. This observation contrasts with what has previously been observed for the reaction of H^+ and $Rh_2(CO)_3(dppm)_2$ (**1**) which yields the μ -H complex **2** instead of a formyl species. The comparative instability of a formyl species may account for this difference. Complex **3** is fluxional and undergoes reversible deinsertion and loss of CO at room temperature. Based on spectroscopic and structural evidence, the μ -acetyl carbon in this species has significant carbene-like character and may be described as a metalla-oxo-stabilized carbene. We find that complex **3** also reacts with excess CO to generate $Rh_2(CH_3CO)(CO)_3(dppm)_2^+$ *in situ*. Conversely, at higher temperatures, complex **3** loses CO to form the dicarbonyl A-frame species $Rh_2(CH_3)(\mu-CO)(CO)(dppm)_2^+$ (**4**). In solution, complex **4** is fluxional and believed to undergo facile methyl migration between metal centers. The unsymmetrical A-frame structure of **4** is confirmed by a single crystal structure determination which clearly shows the presence of a terminal methyl group.

Supplementary material

Complete listings of crystallographic details, bond lengths and bond angles, positional and anisotropic thermal parameters for **3** and **4** are available from the authors on request.

Acknowledgements

We thank the National Science Foundation (CHE-89-09060) for financial support of this work, and Johnson Matthey Co. for a generous loan of rhodium trichloride. We also thank Dr Glen Rosini and Mr Brian Cleary for help with different aspects of the study.

References

- 1 K.W. Kramarz, T.C. Eisenschmid, D.A. Deutsch and R. Eisenberg, *J. Am. Chem. Soc.*, **113** (1991) 5090–5092.
- 2 C.P. Kubiak, C. Woodcock and R. Eisenberg, *Inorg. Chem.*, **21** (1982) 2119–2129.
- 3 J.T. Mague and A.R. Sanger, *Inorg. Chem.*, **18** (1979) 2060–2066.
- 4 L. Manojlovic-Muir, K.W. Muir, A.A. Frew, S.S.M. Ling, M.A. Thomson and R.J. Puddephatt, *Organometallics*, **3** (1984) 1637–1645.
- 5 S. Muralidharan and J.H. Espenson, *J. Am. Chem. Soc.*, **106** (1984) 8104–8109.
- 6 R. Puddephatt, *J. Chem. Soc. Rev.*, **12** (1983) 99.
- 7 P.R. Sharp and J.R. Flynn, *Inorg. Chem.*, **26**(1987) 3231–3234.
- 8 B.R. Sutherland and M. Cowie, *Organometallics*, **4** (1985) 1801–1810.
- 9 B.A. Vaartstra, K.N. O'Brien, R. Eisenberg and M. Cowie, *Inorg. Chem.*, **27** (1988) 3668–3672.
- 10 B.A. Vaartstra and M. Cowie, *Inorg. Chem.*, **28** (1989) 3138–3147.
- 11 C. Woodcock and R. Eisenberg, *Inorg. Chem.*, **23** (1984) 4207–4211.
- 12 M.L. Kullberg and C.P. Kubiak, *Inorg. Chem.*, **25** (1986) 26–30.
- 13 D.M. Hoffman and R. Hoffmann, *Inorg. Chem.*, **20** (1981) 3543–3555.
- 14 B. Delavaux, B. Chaudret, N.J. Taylor, S. Arabi and R. Poilblanc, *J. Chem. Soc., Chem. Commun.*, (1985) 805.
- 15 M. Cowie and S.J. Loeb, *Organometallics*, **4** (1985) 851–857.
- 16 M. Cowie and S.K. Dwight, *Inorg. Chem.*, **19** (1980) 2508–2513.
- 17 A.L. Balch, L.S. Benner and M.M. Olmstead, *Inorg. Chem.*, **18** (1979) 2996–3003.
- 18 A.L. Balch, C.L. Lee, C.H. Lindsay and M.M. Olmstead, *J. Organomet. Chem.*, **177** (1979) C22–C26.
- 19 M. Cowie, S.K. Dwight and A.R. Sanger, *Inorg. Chim. Acta*, **31** (1978) L407–L409.
- 20 K.W. Kramarz and R. Eisenberg, *Organometallics*, **11** (1992) 1997.
- 21 C. Woodcock and R. Eisenberg, *Inorg. Chem.*, **24** (1985) 1285–1287.
- 22 J.T. Mague and J.P. Mitchener, *Inorg. Chem.*, **8** (1969) 119–125.
- 23 S.P. Deraniyagala and K.R. Grundy, *Organometallics*, **4** (1985) 424–426.
- 24 N. Walker and D. Stuart, *Acta Crystallogr., Sect. A*, **39** (1983) 158–166.
- 25 M. Cowie and R.S. Dickson, *Inorg. Chem.*, **20** (1981) 2682–2688.
- 26 S.P. Deraniyagala and K.R. Grundy, *Inorg. Chim. Acta*, **84** (1984) 205–211.
- 27 Y.-W. Ge and P.R. Sharp, *Organometallics*, **7** (1988) 2234–2236.
- 28 Y.-W. Ge and P.R. Sharp, *Inorg. Chem.*, **31** (1992) 379–384.
- 29 W.-D. Wang, S.I. Hommeltoft and R. Eisenberg, *Organometallics*, **7** (1988) 2417–2419.
- 30 Y.-W. Ge, F. Peng and P.R. Sharp, *J. Am. Chem. Soc.*, **112** (1990) 2632–2640.
- 31 G. Erker, *Angew. Chem., Int. Ed. Engl.*, **28** (1989) 397–534.
- 32 U. Schubert, *Coord. Chem. Rev.*, **55** (1984) 261–286.
- 33 K.A. Johnson and W.L. Gladfelter, *Organometallics*, **9** (1990) 2101–2105.
- 34 E.N. Jacobsen, K.I. Goldberg and R.G. Bergman, *J. Am. Chem. Soc.*, **110** (1988) 3706–3707.
- 35 R.B. Calvert and J.R. Shapley, *J. Am. Chem. Soc.*, **99** (1977) 5225–5226.
- 36 F. Antwi-Nsiah and M. Cowie, *Organometallics*, **11** (1992) 3157–3163.
- 37 N.E. Schore, C.S. Ilenda, M.A. White, H.E. Bryndza, M.G. Matturro and R.G. Bergman, *J. Am. Chem. Soc.*, **106** (1984) 7451–7461.
- 38 M.J. Krause and R.G. Bergman, *Organometallics*, **5** (1986) 2097–2108.
- 39 M.K. Reinking, P.E. Fanwick and C.P. Kubiak, *Angew. Chem., Int. Ed. Engl.*, **28** (1989) 1377–1379.